Longitudinal Magnetoresistance in n-Type Germanium: Theoretical*

S. C. MILLER AND M. A. OMAR
University of Colorado, Boulder, Colorado
(Received February 16, 1961)

The longitudinal magnetoresistance of n-type germanium is calculated for high magnetic fields where Landau levels are important. The scattering mechanisms considered are acoustic and ionized impurity scattering. Comparison is made with experiment for acoustic scattering and is found to be satisfactory for sufficiently high fields.

I. INTRODUCTION

EXPERIMENTAL results at high magnetic fields for longitudinal magnetoresistance in n-type germanium have recently been found by Love and Wei.[1] In this paper an attempt is made to explain these results theoretically.

The theory for low magnetic fields has been given by Abeles and Meiboom[2] and Shibuya.[3] In that case one can neglect the Landau[4] quantization due to the magnetic field. For the case of a high magnetic field this quantization has been found to be very important. This was investigated by Argyres and Adams[5] for spherical energy surfaces. There are two criteria for a high magnetic field. One is $\omega^*\tau\gg1$, where ω^* is the cyclotron frequency and τ is the collision time. This criterion means that the Landau states give good basis functions to be used in a perturbation calculation of the electron scattering. It will be discussed in Sec. III. The other, $\hbar\omega^*\gg kT$, means that the magnetic quantization is important in the statistical treatment, i.e., most of the electrons will be in the lowest Landau level. Possibly, from the experimental standpoint, a better combined criterion would be that the magnetic field is large enough to give deviations from the saturation magnetoresistance.

The calculations in this paper are similar to those of Argyres and Adams[5] with the modifications necessary using ellipsoidal rather than spherical energy surfaces. The well-established four-ellipsoid model[6] for the energy surfaces of n-type germanium is used. The only scattering mechanisms considered are acoustic and ionized impurity scattering. The unperturbed wave functions based on a high magnetic field are given in Sec. II along with some useful matrix elements utilizing these functions. In Secs. III and IV these matrix elements are used to get transition probabilities from which relaxation times are found. The Boltzmann transport equation is used to calculate the perturbed distribution function, which then gives the conductivity. The longitudinal conductivity is calculated in Sec. III for acoustic scattering and in Sec. IV for ionized impurity scattering. These are found numerically only for the ⟨100⟩, ⟨110⟩, and ⟨111⟩ directions for the fields. For other orientations without the symmetry properties of these directions, induced transverse voltages resulting from the anisotropy should be taken into account.

II. WAVE FUNCTIONS

In the effective-mass approximation, the Hamiltonian for an electron in an anisotropic crystal in the presence of a magnetic field is

$$\mathcal{H}=\sum_{ij}\alpha_{ij}(p_i+eA_i/c)(p_j+eA_j/c)/2m, \qquad (1)$$

where A_i is a component of the vector potential, and α_{ij}/m is the reciprocal mass tensor. The interaction between the electron and the scattering mechanism is neglected in this Hamiltonian and is treated as a perturbation in Secs. III and IV. For the special case of germanium the energy surfaces are ellipsoids of revolution with the longitudinal principal axes along the ⟨111⟩ directions. Only one ellipsoid is considered in the intermediate calculations. When the final results are obtained, the appropriate summation over the four ellipsoids is made. If the y axis is taken perpendicular to the longitudinal principal axis of an ellipsoid, the components of the α tensor are

$$\begin{aligned}
&\alpha_{11}=\alpha_1\cos^2\theta+\alpha_3\sin^2\theta,\\
&\alpha_{22}=\alpha_1,\\
&\alpha_{33}=\alpha_1\sin^2\theta+\alpha_3\cos^2\theta,\\
&\alpha_{12}=\alpha_{21}=\alpha_{23}=\alpha_{32}=0,\\
&\alpha_{13}=\alpha_{31}=(\alpha_1-\alpha_3)\sin\theta\cos\theta,
\end{aligned} \qquad (2)$$

where m/α_3 is the longitudinal mass and m/α_1 is the transverse mass. The angle θ is measured between the z axis and the longitudinal principal axis.

For a uniform magnetic field H in the positive z direction, take

$$A_x=A_z=0, \quad A_y=Hx. \qquad (3)$$

The gauge has been chosen in order to have the Schrödinger equation separable. Solutions of the equation are then of the form

$$\psi_{n,k}=\phi_n[\beta(x+\lambda^2k_y)]\exp[-i\gamma k_z x+i(k_y y+k_z z)], \qquad (4)$$

* This work supported by the U. S. Army Office of Ordnance Research.

[1] W. F. Love and W. F. Wei, preceding paper [Phys. Rev. **123**, 67 (1961)].
[2] B. Abeles and S. Meiboom, Phys. Rev. **95**, 31 (1954).
[3] M. Shibuya, Phys. Rev. **95**, 1385 (1954).
[4] L. Landau, Z. Physik **64**, 629 (1930).
[5] P. N. Argyres and E. N. Adams, Phys. Rev. **104**, 900 (1956).
[6] G. Dresselhaus, A. F. Kip, and C. Kittel, Phys. Rev. **95**, 568 (1954).

with energies referred to the bottom of the conduction band,

$$\epsilon_{n,k}=(n+\tfrac{1}{2})\hbar\omega^*+\hbar^2k_z^2/2m^*, \quad n=0, 1, 2, \cdots. \quad (5)$$

Here ϕ_n is the Hermite function

$$\phi_n=(\beta/\pi^{\frac{1}{2}}2^n n!)^{\frac{1}{2}}H_n[\beta(x+\lambda^2k_y)] \times\exp[-\tfrac{1}{2}\beta^2(x+\lambda^2k_y)^2], \quad (6)$$

where H_n is a Hermite polynomial. The functions are normalized in a unit cube. The following notations are used here and in the rest of the paper:

$$\omega=eH/mc, \qquad \lambda=(c\hbar/eH)^{\frac{1}{2}},$$
$$\omega^*=\omega(\alpha_1\alpha_{11})^{\frac{1}{2}}, \qquad \beta=\alpha_1^{\frac{1}{4}}/(\lambda\alpha_{11}^{\frac{1}{4}}),$$
$$m^*=m\alpha_{11}/\alpha_3\alpha_1, \qquad \gamma=\alpha_{13}/\alpha_{11}.$$

The quantity ω is the free electron cyclotron frequency, ω^* is the actual cyclotron frequency, and m^* is the effective translational mass along the z axis.

In Sec. III it will be shown that one needs only the diagonal elements of the current operator for the eigenstates of Eqs. (4) and (5). These are

$$\langle n,k|J_x|n,k\rangle=\langle n,k|J_y|n,k\rangle=0,$$
$$\langle n,k|J_z|n,k\rangle=-e\hbar k_z/m^*. \quad (7)$$

Also, for calculation of the scattering probability between different states, the matrix elements of $\exp(i\mathbf{q}\cdot\mathbf{r})$ between these states are needed. Using Eq. (4), one finds

$$\langle n',k'|\exp(i\mathbf{q}\cdot\mathbf{r})|n,k\rangle=(2\pi)^{-2}\delta(k_y'-k_y-q_y) \times\delta(k_z'-k_z-q_z)M_{n',n}(q_x,q_z,k_y,k_y'), \quad (8)$$

where $M_{n',n}$ is the matrix element,

$$M_{n',n}(q_x,q_z,k_y,k_y')=\int dx\,\phi_{n'}[\beta(x+\lambda^2k_y')] \times\phi_n[\beta(x+\lambda^2k_y)]\exp[i(q_x+\gamma q_z)x]. \quad (9)$$

One can use the generating function of the Hermite polynomials to establish

$$M_{n',n}(q_x,q_z,k_y,k_y')=\sum_s 2^{s-\frac{1}{2}(n+n')}(n!)^{\frac{1}{2}}(n'!)^{\frac{1}{2}} \times[(n-s)!(n'-s)!s!]^{-1}[-\beta\lambda^2q_y+i\beta^{-1}(q_x+\gamma q_z)]^{n-s} \times[\beta\lambda^2q_y+i\beta^{-1}(q_x+\gamma q_z)]^{n'-s}\exp[-\tfrac{1}{4}(\beta\lambda^2q_y)^2 -\tfrac{1}{4}\beta^{-2}(q_x+\gamma q_z)^2-\tfrac{1}{2}i\lambda^2(q_x+\gamma q_z)(k_y+k_y')], \quad (10)$$

where the summation over s is from zero to the smaller of n and n'. Equation (9) leads to the result[7]

$$\int dq_xdq_y|M_{n',n}|^2=2\pi/\lambda^2. \quad (11)$$

III. CONDUCTIVITY FOR ACOUSTIC SCATTERING

The perturbation Hamiltonian due to lattice vibrations is taken to be

$$H_i=E\sum_q Q_q q\exp(i\mathbf{q}\cdot\mathbf{r}), \quad (12)$$

where E is the coupling constant between the electrons and the dilational waves of the Shockley-Bardeen theory.[8] Scattering by shear waves is not considered here.

The transition probability from state n, k to state n', k' due to this Hamiltonian is

$$W(n,k;n',k')=(\pi E^2/\rho u_L)\sum_q|\langle n',k'|\exp(i\mathbf{q}\cdot\mathbf{r})|n,k\rangle|^2 \times q[(N_q+1)\delta(\epsilon_{n',k'}-\epsilon_{n,k}+\hbar\omega_q) +N_q\delta(\epsilon_{n',k'}-\epsilon_{n,k}-\hbar\omega_q)], \quad (13)$$

where ρ is the mass density, u_L is the longitudinal speed of sound, N_q is the number of phonons of propagation vector q, and ω_q is the angular frequency of the phonon. For a semiconductor such as germanium and for the temperatures of interest here, $T>15°$K, $\hbar\omega_q$ is smaller than the electron energy for most electrons and therefore it can be dropped from Eq. (13). Also the N_q can be replaced by the high-temperature limit of the Bose-Einstein distribution function, $kT/\hbar\omega_q$. Then Eq. (13) becomes

$$W(n,k;n',k')=AkT\delta(\epsilon_{n',k'}-\epsilon_{n,k}) \times\sum_{q_x}|M_{n',n}(q_x,q_z,k_y',k_y)|^2, \quad (14)$$

with

$$A=2\pi E^2/(\hbar\rho u_L^2). \quad (15)$$

On summing Eq. (14) over k_y' with the help of Eq. (11), one obtains

$$W(n,k_z;n',k_z')\equiv\sum_{k_y'}W(n,k;n',k') =AkT\frac{\delta(\epsilon_{n',k'}-\epsilon_{n,k})}{(2\pi\lambda^2)}. \quad (16)$$

It will now be assumed that there is a relaxation time τ such that

$$\tau^{-1}=-\dot{k}_z/k_z. \quad (17)$$

The time rate of change of k_z in terms of W is

$$\dot{k}_z=\sum_{n',k_z'}W(n,k_z;n',k_z')(k_z'-k_z). \quad (18)$$

Therefore, conversion of the summation in Eq. (18) to an integral over $\epsilon_{n',k'}$ by means of Eq. (5) yields

$$\tau^{-1}=AkT(2m^*)^{\frac{1}{2}}\hbar^{-1}(2\pi\lambda)^{-2}\sum_n'[\epsilon-(n+\tfrac{1}{2})\hbar\omega^*]^{-\frac{1}{2}}. \quad (19)$$

The prime on the summation means that n goes from zero to the largest integer for which $\epsilon-(n+\frac{1}{2})\hbar\omega^*>0$. In the limit as ω^* approaches zero and n becomes large, the summation can be replaced by an integral and Eq. (19) approaches on the average the zero-field expression,

$$\tau^{-1}=AkTm^{\frac{3}{2}}(\alpha_1^2\alpha_3)^{-\frac{1}{2}}\epsilon^{\frac{1}{2}}/(2^{\frac{1}{2}}\pi^2\hbar^3). \quad (20)$$

Kohn and Luttinger[9] have shown how the transport equation can be found from the differential equation giving the time dependence of the density matrix.

[7] V. S. Titeica, Ann. Physik **22**, 129 (1935).

[8] W. Shockley and J. Bardeen, Phys. Rev. **80**, 72 (1950).

[9] W. Kohn and J. M. Luttinger, Phys. Rev. **108**, 590 (1957).

Their procedure in this case gives for the lowest-order approximation,

$$(m^*)^{-1}e\hbar k_z \mathcal{E}\partial f_0/\partial\epsilon = -(\partial f/\partial t)_{\text{collisions}}, \quad (21)$$

in which f_0 is the zero-electric-field distribution function and $\mathcal{E}$ is the electric field. In finding the density matrix, the wave functions of Eq. (4) are perfectly usable, and the condition $\hbar\omega^* \gg 1$ need not be considered. However, Eq. (21) corresponds to retaining only the diagonal elements in the density matrix, i.e., $\Delta n=0$. In this representation for small magnetic fields, the off-diagonal terms of the density matrix where $\Delta n=\pm 1$ are comparable in magnitude to the diagonal terms and give appreciable contribution to the current. These off-diagonal terms are small and can be neglected only if $\omega^*\tau > 1$. This will be assumed in the following. One would expect that this theory and that of Abeles and Meiboom[2] would fit together in their saturation region where the magnitude of $\omega^*\tau$ is on the order of one. The usual procedure for finding f in terms of τ leads to

$$f = f_0 + (m^*)^{-1}e\hbar k_z \mathcal{E}\tau\partial f_0/\partial\epsilon. \quad (22)$$

In relatively pure germanium the statistics are nondegenerate; thus

$$f_0 = \exp[(\mu_H - \epsilon)/kT], \quad (23)$$

where μ_H is the Fermi energy in the presence of the magnetic field H.

The current density $\mathbf{j}$ is given by the trace of the current operator times the density matrix. Since the diagonal elements of the density matrix given by Eq. (21) are predominant, $\mathbf{j}$ is

$$\mathbf{j} = 2(2\pi)^{-2}\sum_n \int \langle n,k|\,\mathbf{J}\,|n,k\rangle f dk_y dk_z. \quad (24)$$

From Eq. (7)

$$j_x = j_y = 0.$$

Also from Eq. (7) it is clear that the integrand is independent of k_y. One can, therefore, integrate at once over k_y obtaining

$$\int_{-1/2\lambda^2}^{1/2\lambda^2} dk_y = 1/\lambda^2. \quad (25)$$

The limits arise from Eq. (4). Gathering together Eqs. (7), (22), (24), and (25), one finds

$$j_z = -2(e\hbar/2\pi\lambda m^*)^2 \mathcal{E}\sum_n \int k_z^2 dk_z\, \tau\partial f_0/\partial\epsilon. \quad (26)$$

Equations (5), (19), and (26) then give for the longitudinal conductivity in the magnetic field H

$$\sigma_{zz}(H) = [4e^2(Am^*)^{-1}(kT)^{-2}]\exp\left(\frac{\mu_H}{kT}\right)\int_{\frac{1}{2}\hbar\omega^*}^{\infty} d\epsilon\, e^{-\epsilon/kT} \times \sum_n{}'[\epsilon-(n+\tfrac{1}{2})\hbar\omega^*]^{\frac{1}{2}}\{\sum_n{}'[\epsilon-(n+\tfrac{1}{2})\hbar\omega^*]^{-\frac{1}{2}}\}^{-1}. \quad (27)$$

Also, $\sigma_{xz}(H)$ and $\sigma_{yz}(H)$ are zero to this order of approximation. Anisotropic effects in higher approximations involving off-diagonal matrix elements of the J's could make these quantities different from zero.

The calculations so far have been concerned with a single ellipsoid. To obtain the total conductivity one has to sum $\sigma_{zz}(H)$ over the four ellipsoids. Also the Fermi energy μ_H is needed. This is evaluated in terms of the electron concentration, $N(H)$, as follows. The electron concentration in the νth ellipsoid is

$$N^\nu(H) = 2\sum_n \int f^\nu dk_z/(2\pi\lambda)^2 = (2\pi\lambda)^{-2}\exp(\mu_H/kT)(2\pi m_\nu^* kT/\hbar^2)^{\frac{1}{2}} \times \operatorname{csch}(\hbar\omega_\nu^*/2kT). \quad (28)$$

Hence, summing over the four ν's to obtain the total concentration, one finds

$$\exp(\mu_H/kT) = (2\pi\lambda)^2 N(H)[\sum_\nu (2\pi m_\nu^* kT/\hbar^2)^{\frac{1}{2}} \times \operatorname{csch}(\hbar\omega_\nu^*/2kT)]^{-1}. \quad (29)$$

In the limit as H approaches zero, one obtains the usual Fermi energy for zero field,

$$\exp(\mu_0/kT) = (2mkT/\pi\hbar^2)^{-\frac{3}{2}}(\alpha_1^2\alpha_3)^{\frac{1}{2}}N_0. \quad (30)$$

When Eq. (27) is summed over the four ellipsoids and combined with Eq. (29), the result is

$$\sigma_{zz}(H) = [16\pi^2 e^2 N(H)\lambda^2/A] \times [\sum_\nu F(\hbar\omega_\nu^*/kT)\exp(-\tfrac{1}{2}\hbar\omega_\nu^*/kT)/m_\nu^*] \times [\sum_\nu (2\pi m_\nu^* kT/\hbar^2)^{\frac{1}{2}}\operatorname{csch}(\tfrac{1}{2}\hbar\omega_\nu^*/kT)]^{-1}. \quad (31)$$

The function F is given by

$$F(\xi) = \int_0^\infty d\eta\, e^{-\eta}\sum_n{}'[\eta - n\xi]^{\frac{1}{2}}/\sum_n{}'[\eta - n\xi]^{-\frac{1}{2}}. \quad (32)$$

It is easily shown that as ξ approaches infinity, F approaches one. Thus when $\hbar\omega^* \gg kT$, F can be replaced by one in Eq. (31). By properly converting the summations over n to integrals, one can show that in the limit as ξ goes to zero F becomes one-third. The integration in Eq. (32) has been done numerically and an approximate expression for F has been found,

$$F(\xi) \approx 1 - (\tfrac{2}{3} + 0.33\xi + 0.074\xi^2)e^{-\xi}. \quad (33)$$

This has an error of less then $\frac{1}{4}\%$ for $\xi > \frac{1}{2}$. The maximum error of 1% occurs near $\xi = 0.05$ since the slope appears to approach infinity at $\xi = 0$. In any case this differs appreciably from the low ξ expression given by Argyres.[10]

The same calculation will be done for the $H=0$ case since what is frequently measured is $\rho(H)/\rho(0)$, where ρ is the resistivity. The eigenstates and eigenvalues

[10] P. N. Argyres, J. Phys. Chem. Solids 4, 19 (1958).

are now

$$\psi_k=\exp(i\mathbf{k}\cdot\mathbf{r}),$$
$$\epsilon_k=\hbar^2(\alpha_1k_x^2+\alpha_1k_y^2+\alpha_3k_z^2)/2m, \quad (34)$$

in the principal axis system. Using a method similar to that by which Eq. (14) was obtained, one now has

$$W(k,k')=AkT\delta(\epsilon_{k'}-\epsilon_k). \quad (35)$$

Then, using the usual Boltzmann equation with the τ from Eq. (20) and μ_0 from Eq. (30) and summing over the ellipsoids, one obtains for the total conductivity

$$\sigma(0)=(16e^2/9Am)(\alpha_1^2\alpha_3)^{\frac{1}{3}}\times(2\alpha_1+\alpha_3)N_0(2mkT/\pi\hbar^2)^{\frac{3}{2}}. \quad (36)$$

The ratio of the conductivity of Eq. (36) to that of Eq. (31) is

$$\sigma(0)/\sigma_{zz}(H)=(1/9)(2\alpha_1+\alpha_3)[N(0)/N(H)]\times\sum_\nu(\tfrac{1}{2}\hbar\omega_\nu^*/kT)\,\mathrm{csch}(\tfrac{1}{2}\hbar\omega_\nu^*/kT)[\sum_\nu F(\hbar\omega_\nu^*/kT)\times(m/m_\nu^*)\exp(-\tfrac{1}{2}\hbar\omega_\nu^*/kT)]^{-1}. \quad (37)$$

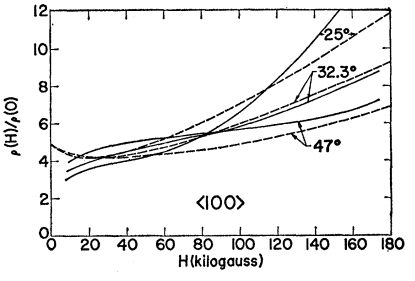

(a)

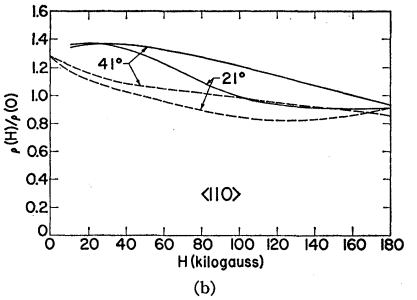

(b)

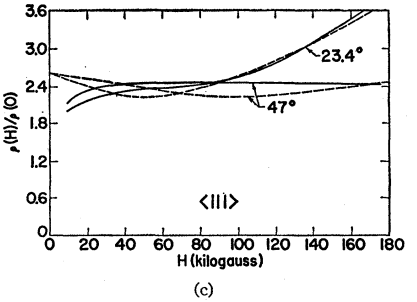

(c)

FIG. 1. Comparison of experimental magnetoresistance of n-germanium with that calculated for acoustic scattering in the ⟨100⟩, ⟨110⟩, and ⟨111⟩ directions. The solid curves are from the experiments of Love and Wei and the dashed curves are the theoretical ones.

This ratio with $N(H)/N(0)$ set equal to one is plotted in Fig. 1 along with the experimental ratio[1] for several directions and temperatures. In the numerical calculations the following values were used:

$$\alpha_1=12.3, \quad \alpha_3=0.63.$$

In the case of large $\hbar\omega^*/kT$, Eq. (37) becomes

$$\sigma(0)/\sigma_{zz}(H)=(1/9)(2\alpha_1+\alpha_3)[N(0)/N(H)]\times(m_\nu^*/m)(\hbar\omega_\nu^*/kT), \quad (38)$$

where the ν refers to the ellipsoid for which ω^* is least. In the low field limit Eq. (37) is

$$\sigma(0)/\sigma_{zz}(H=0)=\tfrac{4}{3}(2\alpha_1+\alpha_3)[\textstyle\sum_\nu m/m_\nu^*]^{-1}. \quad (39)$$

In the isotropic case with $\alpha_1=\alpha_3$ this would be one. However, in general it does not go to one for anisotropic cases as might be expected from the discussion of the transport equation. In fact, Eq. (39) gives the identical ratio that Abeles and Meiboom[2] obtain for the saturation region in their low-field theory. This again suggests that the two theories be connected in this saturation region.

It is clear that Eq. (37) could be used equally well for silicon with obvious modifications of the constants.

IV. CONDUCTIVITY FOR IONIZED IMPURITY SCATTERING

Calculations similar to those of Sec. III will be made in this section for the scattering by ionized impurities. This scattering, of course, predominates in certain temperature and impurity concentration ranges. However, for high magnetic fields the results will indicate that rather high concentrations are needed for it to predominate.

It will be assumed that an electron at $\mathbf{r}$ has a screened Coulomb potential energy due to the ionized center at $\mathbf{R}$,

$$V(\mathbf{r}-\mathbf{R})=-e^2\exp(-k_s|\mathbf{r}-\mathbf{R}|)/K|\mathbf{r}-\mathbf{R}|, \quad (40)$$

where K is the dielectric constant. A semiclassical derivation of the reciprocal screening length k_s is given by Argyres and Adams.[5] It is on the order of 10^5 to 10^6 cm^{-1} for impurity concentrations of 10^{14} to 10^{16} per cm^3 in germanium near 30°K. The Fourier integral for this energy is

$$V(\mathbf{r}-\mathbf{R})=-(e^2/2\pi^2K)\int d\mathbf{q}\exp[i\mathbf{q}\cdot(\mathbf{r}-\mathbf{R})]/(q^2+k_s^2). \quad (41)$$

The transition probability from state n, k to state n', k' from perturbation theory is

$$W(n,k;n',k')=2\pi\hbar^{-1}\textstyle\sum_k|\langle n',k'|V(\mathbf{r}-\mathbf{R})|n,k\rangle|^2\times\delta(\epsilon_{n',k'}-\epsilon_{n,k}). \quad (42)$$

Again using Eqs. (17) and (18) to define the relaxation time and assuming a random distribution of impurities,

one finds

$$\tau^{-1}=-[4e^4N^I(H)/K^2\hbar k_z]\sum_{n'}\int dk_z'dq_xdq_y(k_z'-k_z)$$
$$\times\delta(\epsilon_{n',k'}-\epsilon_{n,k})|M_{n',n}(q_x,q_z,k_y',k_y)|^2$$
$$\times[q_x^2+q_y^2+(k_z'-k_z)^2+k_s^2]^{-2}, \quad (43)$$

where the $M_{n',n}$ are given by Eq. (10) and $N^I(H)$ is the concentration of ionized impurity centers. In this section only the limit $\hbar\omega^*\gg kT$ is considered and therefore only the $n=n'=0$ term will be retained. The integration of this equation over k_z' is readily done because of the delta function. Then the $M_{0,0}$ from Eq. (10) gives

$$\tau^{-1}=[8m^*e^4N^I(H)/\hbar^3K^2|k_z|]\int dq_xdq_y$$
$$\times\exp[-\tfrac{1}{2}(\beta\lambda^2q_y)^2-\tfrac{1}{2}\beta^{-2}(q_x-2\gamma k_z)^2]$$
$$\times(q_x^2+q_y^2+4k_z^2+k_s^2)^{-2}. \quad (44)$$

This integral can be evaluated approximately for large k_z. Let

$$w^2=2(k_z/\beta)^2+\tfrac{1}{2}(k_s/\beta)^2. \quad (45)$$

If w is much greater than one, the integral can be evaluated in an asymptotic power series in $1/w$. In this case the k_s terms can be dropped since over the whole range of interest here $(k_s/\beta)^2$ is very much smaller than one. The resulting τ when only the two leading terms in w are retained is

$$\tau=[\hbar^3K^2\beta^5\lambda^2/2^{\frac{5}{2}}\pi e^4N^I(H)m^*]\{(1+\gamma^2)^2|w|^5$$
$$-[(5\gamma^2-1)-(\beta\lambda)^{-4}(1+\gamma^2)^2]|w|^3\}. \quad (46)$$

Whether or not the large w approximation is good is determined by the exponential in the Boltzmann distribution function. This is a function of the energy ellipsoid orientation. It turns out to be a good approximation for all orientations and magnetic field ranges considered here except for two of the four ellipsoids in the ⟨110⟩ orientation of the fields. For these two ellipsoids the longitudinal axis is perpendicular to the z axis and α_1/α_{11} has its maximum value of 19.4 with $\gamma=0$. An approximate expression for τ in this case accurate to better than 10% over the whole range of w is

$$\tau=[\hbar^3K^2\beta^3|w|/2^{\frac{5}{2}}\pi e^4N^I(H)m^*][4.4w^4+3.6w^2$$
$$+2.5(w^4-w^2)\exp(-5w^2/4)]. \quad (47)$$

Using Eqs. (26) and (29) with the approximation, Eq. (46), one obtains

$$\sigma_{zz}=[64K^2m^*(kT)^3\lambda^2/\pi e^2\hbar^3][N(H)/N^I(H)]$$
$$\times\exp(-\tfrac{1}{2}\hbar\omega^*/kT)\{3(1+\gamma^2)^2-[5\gamma^2-1$$
$$-(\beta\lambda)^{-4}(1+\gamma^2)]\beta^2\hbar^2/4m^*kT\}[\textstyle\sum_\nu(2\pi m_\nu^*kT/\hbar^2)^{\frac{1}{2}}$$
$$\times\operatorname{csch}(\tfrac{1}{2}\hbar\omega_\nu^*/kT)]^{-1}. \quad (48)$$

Similarly, Eq. (47) gives

$$\sigma_{zz}=[64K^2m^*(kT)^3\lambda^2/\pi e^2\hbar^3][N(H)/N^I(H)]$$
$$\times\exp(-\tfrac{1}{2}\hbar\omega^*/kT)[13.2+7.5C^{-4}$$
$$+5(3.6-2.5C^{-3})(C-1)^{-1}/4][\textstyle\sum_\nu(2\pi m_\nu^*kT/\hbar^2)^{\frac{1}{2}}$$
$$\times\operatorname{csch}(\tfrac{1}{2}\hbar\omega_\nu^*/kT)]^{-1}, \quad (49)$$

where

$$C=1+5m^*kT/\beta^2\hbar^2. \quad (50)$$

Here the k_s terms have again been neglected due to their smallness. To obtain the total conductivity the σ's of Eqs. (48) and (49) are summed over the proper ellipsoids.

Finally, these calculations will be repeated for the zero-field case. The transition probability from Eq. (42) is now

$$W(k,k')=32\pi^3e^4N^I(0)\delta(\epsilon_{k'}-\epsilon_k)$$
$$\times\hbar^{-1}K^{-2}[(\mathbf{k}-\mathbf{k}')^2+k_s^2]^{-2}. \quad (51)$$

The relaxation times along the principal directions are now defined as in Eq. (18). There will be one longitudinal relaxation time and two equal transverse times. These are given by

$$\tau_3^{-1}=[2^{\frac{1}{2}}e^4N^I(0)r\alpha_3^{\frac{1}{2}}/K^2m^{\frac{1}{2}}\epsilon^{\frac{3}{2}}]\int d\Omega(1-\cos\theta)$$
$$\times[(1-\cos\theta)^2+r\sin^2\theta+t]^{-2}, \quad (52)$$

$$\tau_1^{-1}=\tau_2^{-1}=[2^{\frac{1}{2}}e^4N^I(0)\alpha_3^{\frac{1}{2}}/K^2m^{\frac{1}{2}}\epsilon^{\frac{3}{2}}]$$
$$\times\int\int d\Omega(1-\sin\theta\cos\phi)[\cos^2\theta(1-r)$$
$$-2r\sin\theta\cos\phi+2r+t]^{-2}, \quad (53)$$

with $d\Omega$ an element of solid angle, $r=\alpha_3/\alpha_1$, and $t=\hbar^2k_s^2\alpha_3/2m\epsilon$. Let the integrals in Eqs. (52) and (53) be called g_3 and g_1, respectively. The integral g_3 can be evaluated in a straightforward manner and the result is

$$g_3=2\pi\left\{(2-r)[(1-r)t-r^2]^{-1}(4+t)^{-1}\right.$$
$$\left.-\tfrac{1}{2}r[(1-r)t-r^2]^{-\frac{3}{2}}\tan^{-1}\left(\frac{2[(1-r)t-r^2]^{\frac{1}{2}}}{(t+2r)}\right)\right\}, \quad (54)$$

for $(1-r)t-r^2$ greater than zero. This condition is satisfied for the energy of the order of kT. The other integral g_1 is not so simple. However, for small r and t the main contribution to the integral is near $\theta=\pi/2$. This suggests that one let $\cos\theta=x$ and then let the limits on x go from minus infinity to plus infinity. Numerical integration shows that in the worst case this leads to an error of about 2%. The integration over ϕ is straightforward, and the integration over x

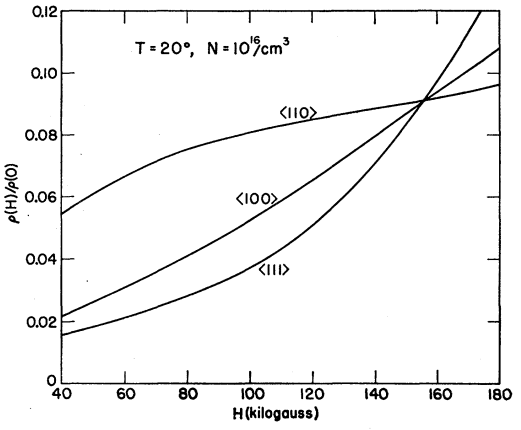

FIG. 2. Calculated magnetoresistance of n-germanium at 20°K and an impurity concentration of 10^{16} per cm^3 for ionized impurity scattering in the ⟨100⟩, ⟨110⟩, and ⟨111⟩ directions.

leads to elliptic integrals. The result is

$$g_1=4\pi[t^{\frac{3}{2}}(1-r)^3ab^2(a^2-b^2)^2]^{-1}\{[a^2+b^2-2(1+r)a^2b^2]\mathbf{E}[(1-b^2/a^2)^{\frac{1}{2}}]-b^2[2-(1+r)(a^2+b^2)]\mathbf{K}[(1-b^2/a^2)^{\frac{1}{2}}]\}, \quad (55)$$

where

$$(1-r)^2a^2=1-r+2rt^{-1}\{1+[1+t(1-r)]^{\frac{1}{2}}\},$$
$$(1-r)^2b^2=1-r+2rt^{-1}\{1-[1+t(1-r)]^{\frac{1}{2}}\}.$$

$\mathbf{K}$ and $\mathbf{E}$ are complete elliptic integrals of the first and second kind, respectively.

The use of the Boltzmann equation and Eq. (30) gives

$$\sigma_3=\sqrt{2}\alpha_3^{\frac{1}{2}}K^2(kT)^{\frac{3}{2}}[\pi^{\frac{1}{2}}re^2m^{\frac{1}{2}}g_3(3kT)]^{-1}, \quad (56)$$

$$\sigma_1=\sigma_3g_3(3kT)[rg_1(3kT)]^{-1}. \quad (57)$$

Here, g_1 and g_3 are assumed to be slowly varying functions of energy, so they are treated as constants evaluated at an energy $3kT$ which is the maximum of the rest of the integrand. Actually for large enough $N(0)/T$ this assumption is not correct, but nevertheless it leads to a fair approximate value for $\sigma(0)$. The total conductivity is found by summing over the ellipsoids. It is

$$\sigma(0)=\tfrac{4}{3}\sqrt{2}\alpha_3^{\frac{1}{2}}K^2(kT)^{\frac{3}{2}}[1+2g_3(3kT)/rg_1(3kT)]\times[(\pi m)^{\frac{3}{2}}re^2g_3(3kT)]^{-1}. \quad (58)$$

The ratio $\rho_{zz}(H)/\rho(0)$ is plotted in Fig. 2 for the three symmetry directions.

V. CONCLUSION

Comparison of the curves of Fig. 1 indicates that there is reasonably good quantitative agreement between the theory and experiment for $\hbar\omega^*/kT$ greater than 2 if ω^* is the smallest cyclotron frequency for a given direction. For the ⟨100⟩, ⟨110⟩, and ⟨111⟩ directions, respectively, this $\hbar\omega^*/kT$ is $0.99H/T$, $0.37H/T$, and $0.65H/T$ with H in kilogauss. Certainly the agreement is as good as can be expected, considering the difficulty of the experiments and the approximations of the theory. There is qualitative agreement and fair quantitative agreement to lower fields. The minima in the theoretical curves for the ⟨100⟩ direction which do not occur in the experimental curves reflect the increase in $F(\hbar\omega^*/kT)$ with H. The same effect would be predicted for the isotropic case. This occurs at the low fields where the theory cannot be expected to be correct and experimentally the effect probably would not occur in the isotropic case either.

The minima in the ⟨110⟩ direction result from a quite different reason. This is the quantum transfer effect in which electrons in ellipsoids of low mobility shift to ellipsoids of higher mobility. This is due to the changing distribution function when the ground states of the ellipsoids are separated as the magnetic field increases. Mathematically it results primarily from the hyperbolic cosecant term in the numerator of Eq. (37), which in turn comes from the expression for the Fermi energy, Eq. (29). The minima in the ⟨111⟩ direction are due to a combination of these two effects. Experimentally there are very slight minima for this direction for some curves.

While curves for temperatures near 25°K are compared in Fig. 1, these should be regarded with suspicion since there are obviously some other large effects taking place near this temperature. This is especially evident in the large difference between the 25° and 23.4° curves of Fig. 4 in the paper of Love and Wei. It would be desirable to have measurements to higher fields to more carefully check the theory for the higher temperatures.

It should be noted that the ratio $N(H)/N(0)$ was taken to be one in the curves of Fig. 1. There is no real indication that it should be different from this. This would indicate that possibly the theory of Yafet, Keyes, and Adams[11] is not applicable here. It would predict a much lower electron concentration ratio and thus a higher resistivity ratio.

The curves of Fig. 2 are valid only above about 80 kgauss since it was assumed in their derivation that $\hbar\omega^*/kT$ was large compared to one. These curves indicate that the effects of ionized impurity scattering are greatly cut down by the magnetic field. This could give minima in the resistivity for all directions. This effect occurs for several reasons. The potential favors low angle scattering while, because of the magnetic field, $k_z'=-k_z$ gives the relaxation. These competing processes considerably cut down the scattering relative to the zero field scattering. Also, especially for the ⟨100⟩ and ⟨111⟩ directions, the γ in Eq. (44) gives an anisotropic increase in $\sigma_{zz}(H)$. Only the q_x near $2\gamma k_z$ contribute appreciably to the scattering, which again tends to cut down low-angle scattering. Numerical estimates show that for an impurity concentration of

[11] Y. Yafet, R. W. Keyes, and E. N. Adams, J. Phys. Chem. Solids **1**, 137 (1956).

about 10^{15} per cm^3, ionized impurity scattering slightly dominates for zero magnetic field and for temperatures around 30°K, but that at high magnetic fields the acoustic scattering is predominant. The curves of Love and Wei for the doped sample appear to agree with this. The curves are similar to those for the pure samples except that the resistivity ratio is cut down by a factor due to the higher resistivity at zero field. Since no samples had a high enough impurity concentration to make ionized impurity scattering predominant at high fields, no experimental curves are drawn in Fig. 2.

In the limit of very high magnetic fields $\rho(H)/\rho(0)$ for ionized impurity scattering saturates. This is seen for the ⟨110⟩ direction from Eq. (49) in which $C-1$ and λ^2 are both proportional to $1/H$. More accurate expressions for τ for the other directions, similar to Eq. (47) for the ⟨110⟩ direction, would lead to saturation for these directions also. In Fig. 2 there is already saturation in the ⟨110⟩ direction and with only slightly higher fields there will be saturation in the ⟨111⟩ direction. The saturation in the ⟨100⟩ direction will not occur until the magnetic field is four or five times as large, so there is a considerable range in which there is a linear change with H. $\rho(H)/\rho(0)$ is approximately a function of H/T so this saturation occurs at higher fields for higher temperatures.

PHYSICAL REVIEW VOLUME 123, NUMBER 1 JULY 1, 1961

Adiabatic Demagnetization with Yttrium-Rare Earth Alloys*

DAVID T. NELSON† AND SAM LEGVOLD
Institute for Atomic Research and Department of Physics, Iowa State University, Ames, Iowa
(Received February 27, 1961)

Alloys of yttrium with 0.3 and 1.0 atomic percent gadolinium, 1.0 at. % dysprosium, and 0.6 and 1.0 at. % holmium have been investigated to determine their usefulness as the working substance for adiabatic demagnetization. In addition, single crystals of 0.6 and 1.0 at. % holmium-yttrium alloys were studied. Those alloys which exhibited paramagnetic susceptibility behavior in the temperature range 1.2–4.2°K were demagnetized adiabatically from about 11 koe and 1.25°K. The lowest temperature attained was 0.76°K for the single crystal of 1.0 at. % holmium with the magnetic field parallel to the a axis of the hexagonal crystal. Magnetization measurements obtained for the single crystals in the temperature range 1.2–4.2°K indicated strong anisotropy with the a axis as the easy axis of magnetization. Hysteresis was observed in the magnetization of the 1.0 at. % holmium single crystal with the a axis parallel to the field. Entropy removal during magnetization was calculated from the magnetization data for the single crystals and found to be only about 15% of that expected if the alloy behaved like an ideal paramagnetic substance.

INTRODUCTION

THE use of thorium-dysprosium metal alloys in magnetic cooling to obtain temperatures less than 1°K has recently been reported by Parks and Little.[1] We report here the results of adiabatic demagnetizations and susceptibility and magnetization measurements on dilute alloys of rare-earth metals in yttrium.

The work was initiated because of the thermal-contact advantages metal alloys would have over conventional salts. Normally with a metal, one might expect eddy-current heating when demagnetizing, but the high residual resistivities of our alloys essentially eliminate this problem. Yttrium was chosen as the host metal since it has the same crystal structure and very nearly the same lattice parameters as the solute metals. Gadolinium ($J=S=7/2$), with no orbital moment and 7 unpaired spins, was the first solute metal used. In order to study the effect of the spin of the solute metal on the Curie (or Néel) temperature, dysprosium ($J=15/2$, $S=5/2$) and holmium ($J=8$, $S=2$) alloys were next investigated. The small cooling effect observed during adiabatic demagnetization of the holmium-yttrium alloys prompted a study of the magnetic properties of single crystals of these alloys.

MATERIALS STUDIED

The pure metals used in fabrication of the alloys were prepared in this laboratory by methods previously reported.[2,3] The alloys were made by arc melting together in a helium atmosphere the proper amounts of the constituent metals. The button formed by this process was turned over and remelted several times in order to insure a homogeneous alloy. The samples were shaped by machining on a lathe into the nominal size of 1.5-in. length, by 0.6-in. diam. The alloys investigated consisted of two gadolinium-yttrium alloys with 0.3

* Contribution No. 983. Work was performed in the Ames Laboratory of the U. S. Atomic Energy Commission.
† Present address: Department of Physics, Luther College, Decorah, Iowa.
[1] R. D. Parks and W. A. Little, *Seventh International Conference on Low-Temperature Physics, Toronto, 1960* (University of Toronto Press, Toronto, Canada, 1960), Official Programme, 354–356.
[2] F. H. Spedding and A. H. Daane, J. Am. Chem. Soc. **74**, 2783 (1953).
[3] C. V. Banks, O. N. Carlson, A. H. Daane, V. A. Fassel, R. W. Fisher, E. H. Olson, J. E. Powell, and F. H. Spedding, Atomic Energy Commission Report IS-1, Iowa State University, Ames, Iowa, 1959 (unpublished).